



Automatic Method for Visual Grading of Seed Food Products

Pierre Dubosclard, Stanislas Larnier, Hubert Konik, Ariane Herbulot, Michel Devy

► To cite this version:

Pierre Dubosclard, Stanislas Larnier, Hubert Konik, Ariane Herbulot, Michel Devy. Automatic Method for Visual Grading of Seed Food Products. International Conference on Image Analysis and Recognition ICIAR, Oct 2014, Vilamoura, Portugal, Oct 2014, Vilamoura, Algarve, Portugal. pp.485 - 495, 10.1007/978-3-319-11758-4_53 . hal-01097778

HAL Id: hal-01097778

<https://hal.science/hal-01097778>

Submitted on 22 Dec 2014

HAL is a multi-disciplinary open access archive for the deposit and dissemination of scientific research documents, whether they are published or not. The documents may come from teaching and research institutions in France or abroad, or from public or private research centers.

L'archive ouverte pluridisciplinaire **HAL**, est destinée au dépôt et à la diffusion de documents scientifiques de niveau recherche, publiés ou non, émanant des établissements d'enseignement et de recherche français ou étrangers, des laboratoires publics ou privés.

Automatic method for visual grading of seed food products

Pierre Dubosclard^{1,2}, Stanislas Larnier^{1,2}, Hubert Konik³, Ariane Herbulot^{1,2}
and Michel Devy^{1,2}.

¹ CNRS, LAAS, 7 avenue du colonel Roche, F-31400 Toulouse, France

² Univ de Toulouse, UPS, LAAS, F-31400 Toulouse, France

³ Laboratoire Hubert Curien, Saint-Etienne

Abstract. This paper presents an automatic method for visual grading, designed to solve the industrial problem of evaluation of seed lots. The sample is thrown in bulk onto a tray placed in a chamber for acquiring color image. An image processing method had been developed to separate and characterize each seed. The approach adopted for the segmentation step is based on the use of marked point processes and active contour, leading to tackle the problem by a technique of energy minimization.

1 Introduction

In agriculture, the global grain harvest reached several billion tons each year. Seed producers exchange their crops at a price determined by the quality of their production. This assessment, called grading, is performed for each set on a representative sample. The difficulty of this assessment is to fully characterize the sample. To do so, it is necessary to qualify each of its elements. Historically, this has been performed manually by an operator. This method is exposed to various problems and the results can vary from one operator to another.

Alpha MOS company [2] develops systems for quality control of food products. It proposes a visual sensory system to provide an alternative to human evaluation. The assessment should be simple to implement and at least as fast as the human evaluation.



Fig. 1: Image of wheat seeds in bulk.

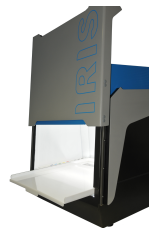


Fig. 2: Acquisition system.

The seed samples are presented in bulk, without any arrangement, but they are spread over a tray in such way that there is no overlapping between the objects to avoid occlusion (Figure 1).

The evaluation by the instrument is composed of three steps. The first step is the **acquisition**: the operator places the samples on the tray in the instrument and takes an image. Then the **detection** step consists in finding each object in the image, to finally classify them in different quality classes regarding several criteria (shape, color, spot) during the **classification** step.

The quality of the sample can then be deduced from the result of the classification. The detection step is the main difficulty. It is necessary to develop a segmentation method to isolate each object under the following constraints:

- the number of seeds is unknown (an approximative estimation can be done);
- the objects have quite generical geometric and chromatic features;
- they are randomly placed, without arrangement and with no overlapping.

In Section 2, a state of the art around the visual grading problem is presented. Section 3 describes the data acquisition system. The notion of marked point processes is introduced in Section 4. The segmentation steps are detailed in Section 5. Numerical results are presented in Section 6.

2 State of the art

Several studies have been conducted on the cereal seeds grading. Augustin et al. [1] focused on the quality control of grain of rice, regarding different criteria of shape and color. From these criteria, a classification method based on neural network is used to qualify each grain. This approach gives good results for the classification of complete, broken and colors defect rice grain. However this method is applied on images with separated grain. The segmentation issue is then simplified by an operator or a mechanical system (vibrating bowl or slot) to separate the grain in front of the camera.

Other studies have been conducted on the cereal segmentation topic, mainly on wheat and rice. Yao et al. [12] and Faessel et al. [8] focused on detection and separation of rice grain. They both address the problem by working on a binary image obtained by a threshold to separate the objects from the background. Yao et al. [12] then work on the contours and search the concaves angles to connect them two at a time in order to detect objects boundaries. Faessel et al. [8] used a mathematical morphology method on the binary image: a skeleton operation on the background. The open lines of the skeleton, without ending, are then combined under some constraints to obtain the objects boundaries. These two methods give good results on image of touching grain with low density of objects. The computation times are short, but these methods are not adapted for images with heaps and high density of seeds.

3 Acquisition system

The acquisitions are made in a cabin (Figure 2) which integrates a camera and a lighting system. This cabin offers stable and reproducible acquisition condition, independently from the external lighting.

Some improvements have been made on the existing system available at Alpha MOS. The lighting system and the camera have been replaced by new material to improve the quality and the stability of the color image acquisition. The lighting source retained is composed of white LEDs. These LEDs have a continuous spectrum in the visible range and were chosen for their stability over time in term of luminous intensity. As LEDs are punctual sources, a diffuser is placed downstream to ensure the lighting homogeneity in the acquisition area. The image acquisition is performed at a distance of 400 mm from the object plan by a CMOS mono sensor color camera of 5 megapixel with a 5 mm lens. The chosen camera was a Basler acA2500-14gc. It offers a resolution on the object plan around 6 pixels per millimeter, which is important for our application as the objects have a size of only few millimeters. The image acquisitions presented in this paper were obtained with this system.

4 Marked point processes

The notion of marked point processes has widely been used to represent stochastic phenomena such as waiting queue. More recently, this approach was used to extract objects in image processing with for example, the detection of roads [9] or to count trees [11] on satellite and aerial images.

4.1 Introduction to the marked point processes

Figure 1 presents an example of seeds. The chosen approach to modelize and extract the seeds is based on the marked point processes. Indeed, the seeds can be represented by a generical simple shape and there is no arrangement between them, they are randomly disposed. These objects are defined by their positions and their geometric attributes or marks. Let χ be the space of objects such as $\chi = P \times M$, with P the space of the position and M the space of the geometric attributes describing the object. A configuration of objects from χ , noted \mathbf{x} , is a non-arranged list of objects: $\mathbf{x} = \{x_1, \dots, x_n\}, n \in \mathbb{N}, x_i \in \chi, i = 1, \dots, n$.

The objects to detect can be approximated by an ellipse characterized by its marks, for example its orientation, its minor axis and its major axis (Figure 3).

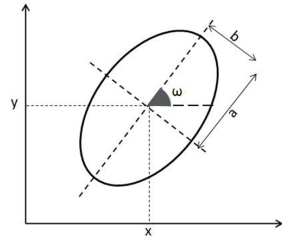


Fig. 3: Position and marks of an ellipse.

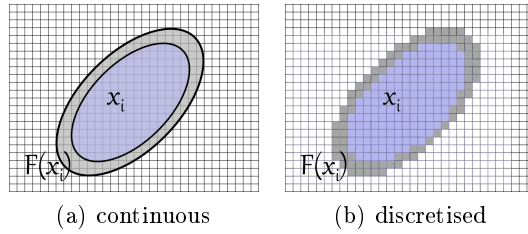


Fig. 4: Object x_i and its crown $\mathcal{F}(x_i)$ (a), and their equivalent discretized (b).

For each object x_i of the configuration \mathbf{x} , an energy $U(x_i)$ composed of two terms is associated. The first term is a *data term* noted $U_d(x_i)$, which represents

the likelihood of the marked point process regarding the data (the image in our case). This term is defined by the data of the object itself. The second term is an *a priori* term, noted $U_p(x_i)$, which imposes condition on the overall configuration.

In the context of object detection inside an image, the aim is to find the most likely object configuration. This research is based on the two energies terms that are defined in the next section.

4.2 Energy $U(\mathbf{x})$

The energy associated to an object x_i , noted $U(x_i)$, is the sum of the data term $U_d(x_i)$ and a priori term $U_p(x_i)$. The energy for the configuration \mathbf{x} is then:

$$U(\mathbf{x}) = U_d(\mathbf{x}) + \gamma U_p(\mathbf{x})$$

with γ a weight coefficient which is determined empirically.

The term $U_d(\mathbf{x})$ takes into account the image data for each object of \mathbf{x} . It is computed by using the Bhattacharyya distance, noted d_B , defined in [6]:

$$d_B(x_i, \mathcal{F}(x_i)) = \frac{(\mu_1 - \mu_2)^2}{4\sqrt{\sigma_1^2 + \sigma_2^2}} - \frac{1}{2} \log \left(\frac{2\sigma_1\sigma_2}{\sigma_1^2 + \sigma_2^2} \right)$$

with an object $x_i \in \chi$ and $\mathcal{F}(x_i)$ the object crown (Figure 4), (μ_1, σ_1) and (μ_2, σ_2) respectively the means and the variances of the radiometric values of the object and its crown.

The computation of this distance provides a criterion that highlights area with important contrast between the object and its crown. It also takes into account the homogeneity of the area. Finally, the term $U_d(\mathbf{x})$ is defined as follows:

$$U_d(\mathbf{x}) = \sum_{x_i \in \mathbf{x}} U_d(x_i) = \sum_{x_i \in \mathbf{x}} \mathcal{Q}(d_B(x_i, \mathcal{F}(x_i)))$$

with $\mathcal{Q}(d_B) \in [-1, 1]$ a quality function which favors or penalizes the objects considering a given threshold d_0 :

$$\mathcal{Q}(d_B) = \left(1 - \frac{d_B}{d_0}\right) \text{ if } d_B < d_0, \quad \mathcal{Q}(d_B) = \exp\left(-\frac{d_B - d_0}{100}\right) - 1 \text{ if } d_B \geq d_0.$$

The objects having an important contrast with their crown ($d_b > d_0$) are then favored and their associated data energy is negative.

The $U_p(\mathbf{x})$ term gives information on the a priori knowledge on the target configuration, like the interactions between the objects. In the context of seed segmentation, $U_p(\mathbf{x})$ is a repulsive term that penalizes the objects overlapping. For each object $x_i \in \chi$, $U_p(x_i)$ is the sum of repulsive strengths emitted by the objects in interaction with x_i , that are in overlapping with x_i . These repulsive strengths are computed by counting the number of pixels that belong to the object x_i and to its neighbouring objects noted $\mathcal{V}(x_i)$:

$$U_p(\mathbf{x}) = \sum_{x_i \in \mathbf{x}} U_p(x_i) \quad \text{with} \quad U_p(x_i) = \sum_{x_j \in \mathcal{V}(x_i)} \mathcal{A}(x_i \cap x_j)$$

and $\mathcal{A}(x_i \cap x_j)$ the common area of x_i and x_j objects.

5 Segmentation

The presented segmentation method is inspired by the multiple Birth-and-Death algorithm described by Descombes et al. in [7]. This approach involved the marked point processes in an optimization framework. But we adapt this approach to treat our segmentation topic by adding a detection step between the birth step and the death step. The difference with the approach of Descombes et al. is that we do not consider the optimization on the entire configuration but on specific objects. We use this Birth-and-Death dynamic as a sampler, the optimization part is realized by an active contour method detailed later. First, the initialization of the method is presented, then the different steps of the method are described.

5.1 Initialization



Fig. 5: From left to right : input image and birth map corresponding.

Birth map The first initialization step consists of computing an image that is named birth map. This image has the same size as the input image and it associates to every position p a probability $B(p)$ that there is an object centered at this position.

This image is computed in two steps. The first step consists in a binarization of the input image to separate the objects from the background, pixels of the background are set to zero and the probability associated is null. The second step is the computation of the Euclidean distance to the contours.

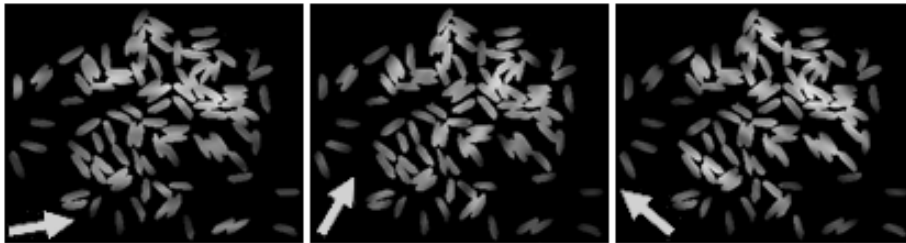


Fig. 6: Example of three orientation maps.

Orientation maps The orientation maps are a set of images that associate to every position different probabilities on the possible orientations of an object in this point. To obtain them, mean filters which have a geometrical shape and different orientations are used on the binary image. The geometrical shape is the mean of the possible shapes which approximate the seeds.

For example, the ellipse had been chosen in the case of rice seeds. Figure 6 presents three orientation maps obtained from the input image in Figure 5.

5.2 Active contour

The objects created in the context of the marked point processes have only simple shapes like ellipses with a limited range of axes sizes. The computational time is the main reason. But to accurately detect every object in the image, we need to obtain the most precise boundaries.

As the objects to detect have a generical shape, we decided to use the method based on an active contour with a geometric shape prior proposed by Bresson et al. [3]. This method follows the well-known energy fonctionnal model of Chen et al. [5] where the shape prior of Leventon et al. [10] is integrated. Finally, to improve the robustness of the method, Bresson et al. add a region-based energy term based on the Mumford-Shah fonctionnal (Vese and Chan [4]). This method is then based on three complementary terms dedicated to shape, boundary and region inside the contour.

5.3 Birth-and-Death dynamic

The method adapted for the Birth-and-Death algorithm is composed of three steps that are done iteratively. We added a detection step to the original approach in order to detect the object boundary with more accuracy, but also to be able to segment the heaps progressively from their boundaries to their cores.

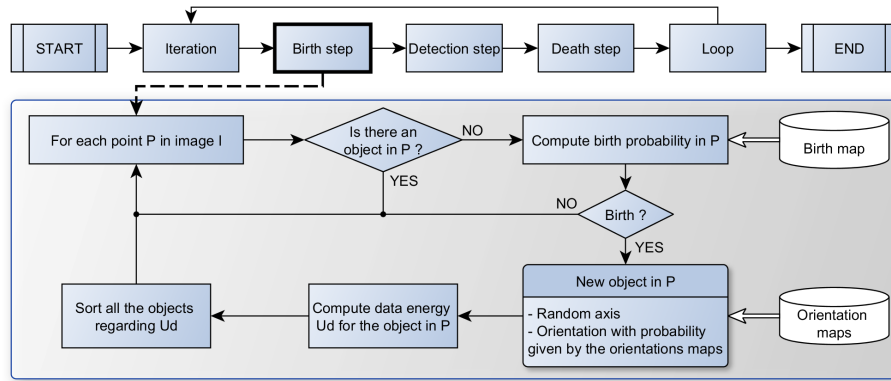


Fig. 7: Birth step.

Birth step The first step consists of objects birth and is illustrated on Figure 7. For each point p of the input image, if there is not already an object at this position, the birth probability $\delta B(p)$ is computed from the birth map, with δ a regularization coefficient that handles the approximative number of objects. If an object x_i is created, its axes are randomly chosen and its orientation is obtained from the set of orientation maps. For a given number of angles, the set of orientation maps provides the probability that an object has this angle. Then the data energy $U_p(x_i)$ of the object x_i is computed and the object is placed in the configuration \mathbf{x} by sorting them regarding their data energy. Once all the image is scanned, the algorithm goes to the next step.

Detection step The aim of the detection step is to validate the objects of the configuration \mathbf{x} . Figure 8 described this step. For each object x_i of the configuration taking by their data energy classement order, their data energy is compared to a threshold. If their energy is inferior to this threshold, they may be correctly placed. Then the active contour approach detailed previously is use to validate this hypothesis on one hand, and to get an accurate boundary if the object is correct on the other hand. The result of the active contour is analyzed to determine different criteria like area or roundness. From these criteria the object is then validated or not. If the object is validated, the object is removed from the configuration \mathbf{x} , the birth map is updated by affecting the probability to create an object in this area at zero. The input image is also updated by turning the pixels values of the correct object to zero, so the heaps can be progressively processed from their boundaries to their cores. If the object is not correct, we only remove it from the configuration \mathbf{x} .

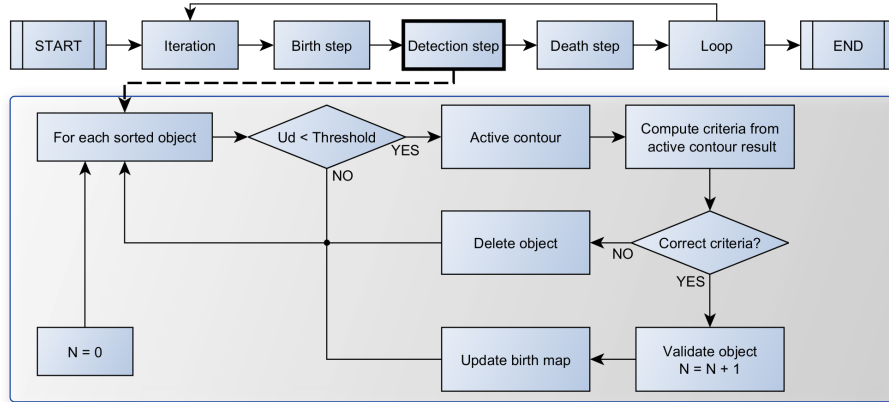


Fig. 8: Detection step.

Death step The death step consists of cleaning the configuration \mathbf{x} and is illustrated on Figure 9. If some object have been validated during the detection step of the current iteration, we compute the new data term of all the objects from the updated input image. We then compute the a priori energy and the death

probability of each object in the configuration:

$$D(x_p) = \frac{\delta a_\varphi(x_p)}{1 + \delta a_\varphi(x_p)} \mathbf{x}$$

with $a_\varphi(x_p) = \exp(-\varphi U(x_p))$. The object is then remove from the configuration with the probability $D(x_p)$.

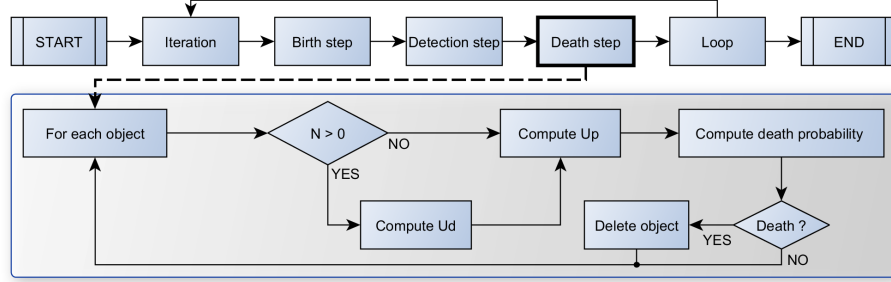


Fig. 9: Death step.

6 Numerical results

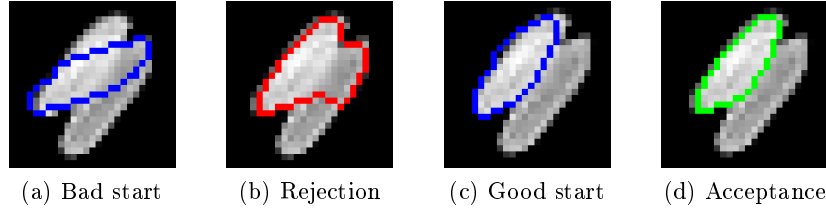


Fig. 10: Behaviour of detection step.

Figure 10 illustrates the behaviour of the detection step in the cases of bad starting contour (a) and a good one (b). The first leads to a final contour with a shape distant from an ellipse and is rejected. The second leads to a final contour with a shape similar to an ellipse and is accepted.

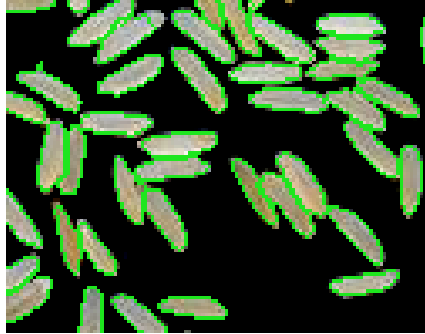
Figure 11 and Figure 12 presents the final segmentation. The green color represents the contours. For the greater part, rice seeds and oats are well detected. Some improvements could be made. Further development is under consideration especially in the algorithm parameters selection. This selection could be made thanks to an automatic learning on separated seed.

7 Conclusion

This paper proposes an approach to perform the visual quality control of cereal seeds samples. This operation called visual grading can be treated in three steps:



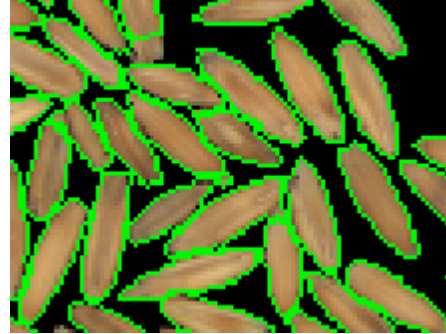
(a) Overall.



(b) Details.



(a) Overall.



(b) Details.

Fig. 11: Final segmentation on rice sam- Fig. 12: Final segmentation on oats sam-
ple. ple.

acquisition, segmentation and classification. An acquisition system of color images has been created to collect the data. A new segmentation approach has been developed, based on the marked point processes. The Birth-an-Death dynamic has been modified to integrate a new detection step based on an active contour with a shape prior term. The results on rice seeds are promising.

Experiments with higher density and with other type of seeds (barley, pea, wheat) are in progress. Other tests like comparison with human operator and reproducibility on the same sample in different configurations are also underway.

In the future, some algorithm parameters will be automatically learnt on simple images with a representation sample of separated seeds. The shape parameters would be extracted from statistics on the binarized image. The integration of a 3D data acquisition system like stereovision with two cameras is under consideration. Despite the hardware cost, such data might be useful in particular to enrich the birth map but also to provide criteria for the classification stage.

8 Acknowledgement

This CIFRE thesis work was made possible thanks to the involment of Alpha MOS company.

References

- [1] O.C. Agustin and Byung-Joo Oh. Automatic milled rice quality analysis. In *Second International Conference on Future Generation Communication and Networking, 2008. FGCN '08*, volume 2, pages 112–115, December 2008.
- [2] Alpha MOS. <http://www.alpha-mos.com>.
- [3] X. Bresson, P. Vandergheynst, and J.-P. Thiran. A variational model for object segmentation using boundary information and shape prior driven by the mumford-shah functional. *International Journal of Computer Vision*, 68(2):145–162, June 2006.
- [4] T.F. Chan and L.A. Vese. Active contours without edges. *IEEE Transactions on Image Processing*, 10(2):266–277, February 2001.
- [5] Y. Chen, H.D. Tagare, S. Thiruvankadam, F. Huang, D. Wilson, K.S. Gopinath, R.W. Briggs, and E.A. Geiser. Using prior shapes in geometric active contours in a variational framework. *International Journal of Computer Vision*, 50(3):315–328, 2002.
- [6] S. Descamps, X. Descombes, A. Bechet, and J. Zerubia. Automatic flamingo detection using a multiple birth and death process. In *IEEE International Conference on Acoustics, Speech and Signal Processing 2008, ICASSP 2008*, pages 1113–1116, Las Vegas, USA, March 2008.
- [7] X. Descombes, R. Minlos, and E. Zhizhina. Object extraction using a stochastic birth-and-death dynamics in continuum. *Journal of Mathematical Imaging and Vision*, 33:136–139, 2009.
- [8] M. Faessel and F. Courtois. Touching grain kernels separation by gap-filling. *Image Analysis and Stereology*, 28(3):195–203, 2011.
- [9] C. Lacoste, X. Descombes, and J. Zerubia. Point processes for unsupervised line network extraction in remote sensing. *IEEE Transactions on Pattern Analysis and Machine Intelligence*, 27(10):1568–1579, 2005.
- [10] M.E. Leventon, W. E L Grimson, and O. Faugeras. Statistical shape influence in geodesic active contours. In *IEEE Conference on Computer Vision and Pattern Recognition, 2000*, volume 1, pages 316–323 vol.1, 2000.
- [11] G. Perrin, X. Descombes, and J. Zerubia. A marked point process model for tree crown extraction in plantations. In *IEEE International Conference on Image Processing (ICIP)*, volume 1, September 2005.
- [12] Q. Yao, Y. Zhou, and J. Wang. An automatic segmentation algorithm for touching rice grains images. In *International Conference on Audio Language and Image Processing (ICALIP)*, pages 802–805, November 2010.